SLAC – PUB – 4610
April 1988
(A)

RECENT PROGRESS AT THE STANFORD LINEAR COLLIDER*

P. S. BAMBADE

Stanford Linear Accelerator Center, Stanford University, Stanford, California 94309, USA

ABSTRACT

A status report on SLC commissioning is given, with special emphasis on recent progress in the Arcs and Final Focus.

INTRODUCTION

The Stanford Linear Collider (SLC) has two main goals [1]. The first is the production of high luminosity electron-positron collisions for studying the physics of the Z^0. The second is to test linear colliders as a new approach towards future high-energy machines.

Circular colliders, where counter-rotating electrons and positrons are stored, are not easily extrapolated to very high energy because of copious synchrotron radiation emitted in the bends. Both size and cost scale [2] as E^2 for an optimized design. Linear colliders avoid this by accelerating beams in linacs to the desired energy and by aiming them at each other on each pulse. More favorable scaling is predicted, but not fully established, and new problems exist. Besides the acceleration mechanism, a special challenge is the small collision point beam size needed to make up in the luminosity for low crossing rate. At the SLC, it is about 2 μm in radius. Both elaborate optics and emittance reductions via radiation damping are required. Considerable effort is also needed to preserve and control phase-space through the system. The SLC, serving to explore such problems, is an important learning experience.

PROJECT OVERVIEW

Table 1 shows the basic parameter specifications [3,4]. The design luminosity is ambitious and will take several years to reach. Initial parameters are projections based on recent progress. Fortunately, even a thousandth of the design luminosity allows to do some interesting physics.

Table 1. Basic parameters for the SLC.

	Design Goal	Initial Goal	Achieved	Units
Beam energy at IP	50	46	46	GeV
Beam energy at end of linac	51	47	53	GeV
Electrons at entrance of arcs	7×10^{10}	10^{10}	3.5×10^{10}	
Positrons at entrance of arcs	7×10^{10}	10^{10}	0.9×10^{10}	
Repetition rate	180	120 Hz	10 Hz	Hz
Normalized transverse emittance at end of linac (electrons)	3×10^{-5}	10×10^{-5}	$3\text{–}10 \times 10^{-5}$	rad-m
Spot radius at IP	1.6	4 μ	~ 4 μ	μm
Luminosity	6×10^{30}	6×10^{27}	–	$\text{cm}^{-2}\,\text{sec}^{-1}$

*Work supported by the Department of Energy, contract DE–AC03–76SF00515.

Invited talk presented at the 19eme Ecole de Physique des Particules, Marseille–Luminy, France, September 7–11, 1987 and at the CERN Accelerator School, Berlin, Germany, September 14–25, 1987

Figure 1 shows the entire SLC complex. Two electron bunches are generated and co-accelerated to 1.2 GeV in the Injector [5]. At 200 MeV, they are joined by a positron bunch. The three are then injected for cooling into two Damping Rings [6], from which they are extracted before the next linac pulse. The existing SLAC Linac has been upgraded [7] and co-accelerates them to 50 GeV. The 6 mm equilibrium ring bunch length is compressed to 1.5 mm before injecting into the Linac in order to minimize wakefield effects there. The last electron bunch is ejected onto a target at 33 GeV, to produce [8,9] positrons. These are returned along the length of the Linac to the 200 MeV point in the Injector. At the end of the Linac, electrons and positrons are brought into collision through two Arcs [1,10]. The Final Focus System [11-13], straddling the interaction area, demagnifies and steers the beams into collision.

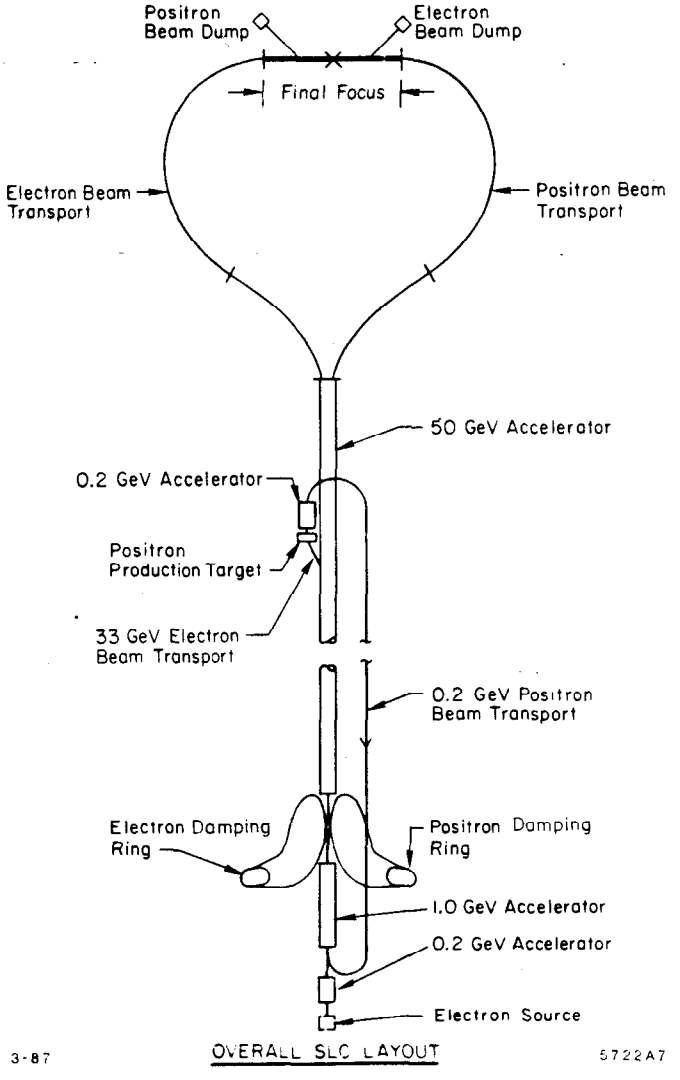

Fig. 1. The Stanford Linear Collider (SLC).

Commissioning and tests of successive stages have been ongoing since the Fall of 1981 and throughout the construction period (Fall 1984 to Spring 1987). Subsequently, much work has been devoted to the newly installed Arcs and Final Focus Systems, with continuing improvements upstream in the Linac, the Electron and Positron Sources, and in the Damping Rings. In this paper, we review the Arcs and Final

Focus activities in detail. The general status of the project, reported on numerous occasions [3,14-18], is briefly summarized.

LINAC AND SOURCES

Injector [5]

The Electron Source and Injector are specified to provide two bunches of 7×10^{10} particles with a momentum spread within the Damping Ring acceptance of $\pm 1\%$. Invariant emittances must be smaller than 180×10^{-5} mrad at 120 Hz operation. These goals are met easily for 5×10^{10} particles per bunch and the system is stabilized through computer controlled feedback.

Damping Rings [6]

The Damping Rings have provided the design invariant emittance of 3×10^{-5} mrad at 1.2 GeV. Both rings are operational but useful current extracted is limited to about 2×10^{10} particles per bunch because of bunch lengthening. The origin of this effect is excessive longitudinal impedance from discontinuities in the vacuum chamber. It is possible to extract larger currents, but the bunches can then not be compressed in the ring to linac transport because of limited aperture. Short-term fixes have included opening up this aperture, and inducing quadrupole oscillations to precompress the bunch within the ring just before extraction.

Some reduction of the impedance can be achieved by installing sleeves inside the bellows, to smooth out the transitions there.

Such fixes are expected to help bring the current up towards the design value. In the short term, the system is adequate for operation at 10^{10} particles per pulse.

Positron Source [8,9]

At 33 GeV in the Linac, the second electron bunch is ejected onto a W-Re target to produce positrons. These are captured in a high gradient acceleration section and confined through solenoidal focusing. They are then transported at 200 MeV back to the beginning of the Linac for reinjection. The biggest issue is to increase the yield of damped positrons reinjected into the Linac per electron incident on the target. Prior to the Fall 1987 shutdown, this yield was down about a factor two due to combined failure of the capture section, which could not be operated at the design 40 MeV/m gradient, and the DC solenoid, which had developed turn-to-turn shorts. This hardware has now been replaced. The solenoid is working properly but the capture section still works more reliably at a reduced gradient. The yield has improved slightly but has not yet been pushed to the design value. 1×10^{10} positron bunches have been obtained at the end of the Linac.

Linac [7]

The Linac has been upgraded with about 200 new 67 MW klystrons [19]. Energies up to 53 GeV have been measured, but running-in is at 47 GeV to produce collisions at the Z^0. Co-acceleration of 10^{10} electrons and positrons is fairly easy and common automated beam guidance is operational. The energy spread can be minimized to .2 to .3%, and work is ongoing to improve launch and energy feedback

stabilization into the Arcs. Optical matching, important to preserve emittances, is underway both at the injection and throughout the lattice. A klystron management program, enabling automatic scaling of the lattice to match to a varying klystron population, is being tested. Invariant emittances between 3 and 10×10^{-5} mrad are at present obtained at the end of the Linac for both beams.

ARCS

Summary of Optics Goals [1,20]

The Arcs are designed to bend the beams without significant dilution of transverse phase-space. Two mechanisms must be counteracted.

The first effect results from *synchrotron radiation*. The photons, emitted at random, cause energy fluctuations. Lower energy particles are bent more and follow curves with shorter average radius. This disperses their trajectories incoherently which enhances horizontal phase-space. Such trajectories execute betatron oscillations in the quadrupole lattice. To minimize the growth, both photon emission rates and oscillation amplitudes must be small [21,22]. This is achieved by making the bending radius large and the betatron period short, through tight focusing. As can be shown [1], the growth is proportional to T_β^3/ρ^4, where T_β is the betatron period and ρ the average radius. Alternating gradient transport modules with the lowest possible field compatible with the SLAC site are therefore used. The packing factor is maximized using combined function magnets, and the lattice chosen to minimize the average invariant amplitude of the dispersed oscillations. For a FODO array, the optimum [23] cell phase-shift to minimize emittance growth is near 135°. For reasons explained below, the adopted design uses 108°. At 50 GeV, the emittance added in one passage is [1] 1.5×10^{-10} rad-m, or one-half of the design value.

The second mechanism for phase-space dilution arises through residual energy spread resulting from the bunch length and the accelerating Linac RF [24]. Because of energy dependance in the focusing, or *chromaticity*, optical distortions from gradient errors are not imaged coherently. For example, an off-energy slice of a mismatched phase-space transmits with a phase-shift $\Delta\psi \approx 2\pi N_\beta \delta_E$ where δ_E is the relative energy error and N_β the number of betatron periods. For a large phase-shift, the overall mismatch averaged over all energies looses its phase relation to the input. The effective volume occupied by the observable phase-space is thereby enlarged. Such *chromatic filamentation* is illustrated in fig. 2, where a normalized phase-space with area one but amplitude two distortion gradually fills up an area of two. With $N_\beta \simeq 70$ in the Arc and for $\sigma_E \simeq 0.5\%$, the spread in betatron phases at the output is about $\sigma_\psi \simeq 0.7\ \pi$.

This effect can be controlled in two ways. In an *active* approach, it is reduced with careful energy spread minimization [7] and good trajectory and optics matching into and through the Arc. In the adopted *passive* approach, sextupoles are used to cancel the chromaticity. Accumulated errors are thus imaged coherently and the final correction can be concentrated in the Final Focus. From a purely optical standpoint, this eases requirements on upstream control. In practice and as we shall explain, much upstream control is still necessary to maintain detectable luminosity.

Sextupoles were introduced by shaping the combined function magnet poles [10]. For the horizontal optics, the vertical component of the magnetic field may be expressed as:

$$B_y(x) = B_o(1 - Qx + Sx^2) \ ,$$

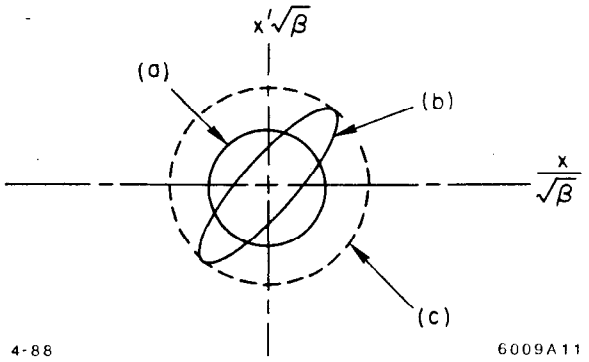

Fig. 2. Nominal phase-space (a), distorted by optical mismatch (b), *filaments* (c) into a larger area when not correcting the chromaticity of the lattice.

where Q and S are the quadrupole and sextupole strengths. The sextupole provides additional focusing for off-energy and off-axis rays with $x = \delta x + \delta_E \eta$, where η is the dispersion function, which suppresses the chromaticity if $2\ S\eta = Q$. Since sine and cosine-like components are equivalent modulo $\pi/2$ in a repetitive lattice, only one family per plane is needed. Additional terms in x^2 and δ^2 for rays solely off-axis or off-energy are suppressed by grouping cells into reasonably local cancellations. *Second-order achromats* [25] achieve this by pairing sextupoles π phase-shift apart into superperiods with the smallest possible multiple of 2π compatible with the cell phase-shift. In the SLC Arcs, each superperiod is 6π, consisting of ten 108° cells. This is a compromise between achromat compactness, best with 90°, and quantum growth, smallest near 135°.

The price to pay for using sextupoles is a lattice sensitive to misalignments. A poorly controlled trajectory generates erect and skew gradient errors through the sextupole which add to magnet imperfections [26] and enhance optical distortions. This lead to stringent magnet to magnet alignment tolerances [20] of about 100 μm.

The efficacy of the chromatic correction was tested by comparing a set of betatron oscillations at two energies. An example of this is shown in fig. 3, where the input beam was deflected horizontally on-energy and 400 MeV off-energy. Overlaying the plots shows nδ phase difference.

Nonplanar Geometry

Commissioning revealed another problem. Although the beam [10] was steered through the North Arc early on with little loss, spots measured at several stages neither reproduced nor agreed with the design, and the beam injected in the Final Focus for hardware tests would not fit in the aperture easily. At times, loss also appeared in the Arc, pointing to suspected mechanical problems with the vacuum chamber or the magnet movers used for steering. In attempts to probe available aperture with beam, it was found that launched oscillations coupled strongly from one plane to the other with growing amplitude (see fig. 4). Measured η also showed coupling and amplification. The origin of this was the nonplanar geometry dictated by strongly varying site elevation, and large installation errors in magnet positioning. Achromats were rolled at their interface to follow the terrain, and big couplings correlated with the largest rolls.

In the original design, rolls were matched in pairs one or more achromats apart for long-range suppression of the coupling, and this was sensitive to deviations in the 6 $n\pi$ phase-advance, from systematic

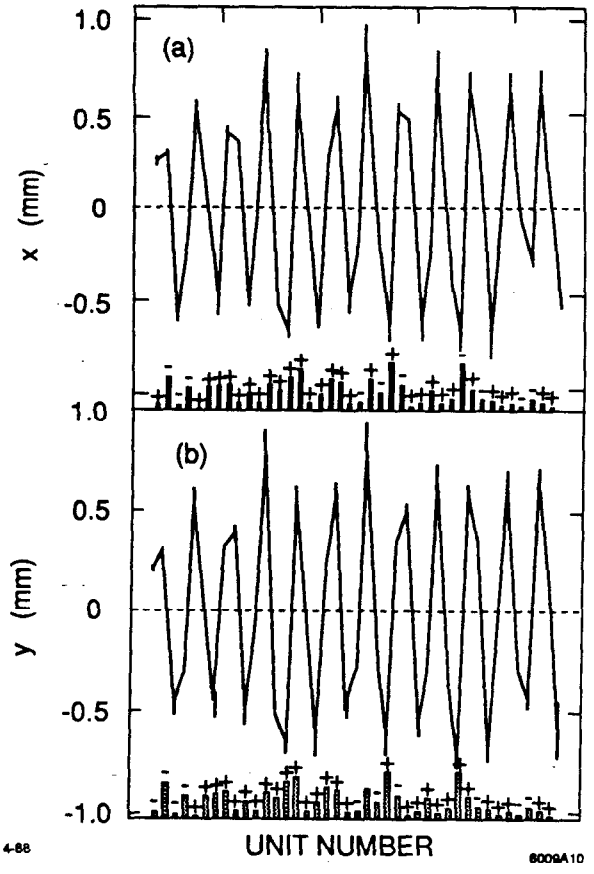

Fig. 3. Betatron oscillation at the end of the Arc, on-energy and 400 MeV off-energy. The chromatic correction suppresses any phase-shift.

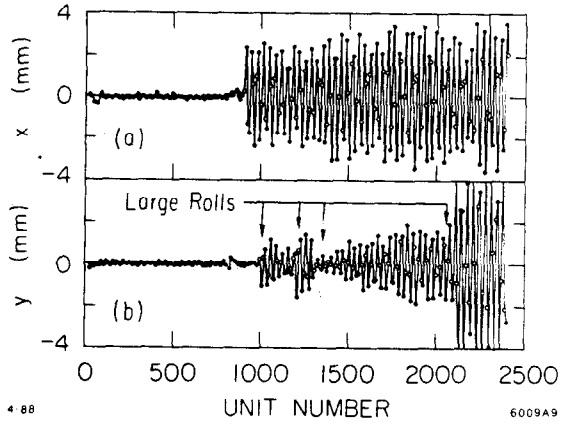

Fig. 4. Cross-coupling of betatron oscillation in the North Arc. Large coupling occurs at the largest rolls.

gradient errors. Such errors initially exceeded the specified design tolerances [1]. Effects can be large as cross-coupling oscillations each time see out of phase optics in the other plane. At a 10° roll, the coupling [27] can be 100%. Overall sensitivity of the betatron size is shown in fig. 5 from TRANSPORT [28], for systematic errors of 3° per cell in each plane. Measured errors were smaller and accounted for a factor three to four overall growth. This was not sufficient to explain the large spots observed in the Final Focus, indicating that the Linac phase-space was not fully controlled.

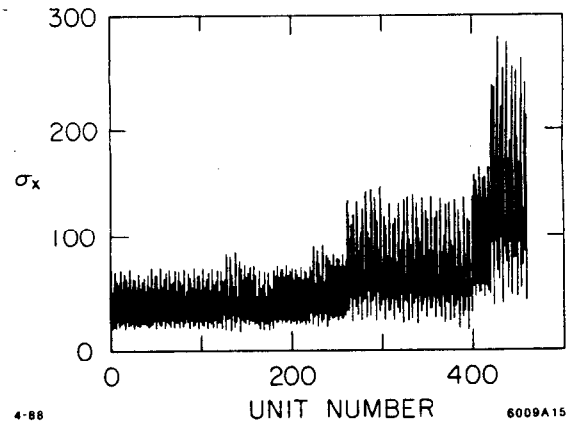

Fig. 5. Growth of betatron spot size in the North Arc, for systematic errors of 3° per cell in each plane.

Phase–Fix and Roll–Fix

Average achromat phase-advances were measured fitting sinusoids to betatron oscillations, and corrected by physically moving magnets, and by combining trim windings in each achromat and a global imbalance between F and D magnets set up in a separate circuit. This *phase-fix*, which was limited by measurement errors, brought errors in the North Arc to within about 0.5° per cell. Overall betatron growth was reduced to a factor 2 and η was essentially matched. The South Arc, only partially corrected, still had large growth. Phase-space injected in the North Final Focus was also reduced, enabling an initial optics program for small IP spots to proceed, but remaining growth, still amplifying variations, would often result in uncorrectable cases.

Splitting up major rolls into smoother transitions was proposed to reduce the sensitivity to systematic gradient errors. It was first found [29] empirically that rolling D lenses near roll transitions by half the total amount suppressed cross-coupling of lattice η. For the betatron motion, an approximate correction scheme was found by splitting rolls in three parts, each a cell apart and with magnitudes satisfying:

$$\theta_{-1}e^{-i2\pi/3} + \theta_0 + \theta_{+1}e^{i2\pi/3} = 0 \ ,$$

as for a matched trajectory bump. Figure 6 illustrates the combined *roll-fix* transition and relative roll ratios. Simulated [30] improvements are shown in fig. 7, for a sample of random and systematic errors, in the as-built and roll-fixed Arcs. Reduction of the growth of spot sizes at the end of the Arc from roll-fix is a factor 1.5 to 2.

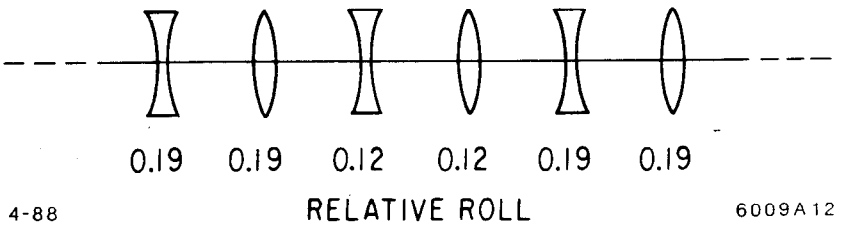

Fig. 6. *Roll-fix* transition.

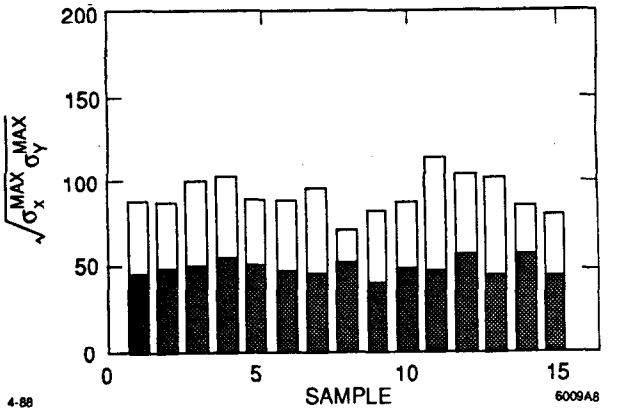

Fig. 7. Growth of betatron size at the end of the Arc, for as-built (white area) and roll-fixed (shaded area) lattice.

Present Status and Plans

Both Arcs have been roll-fixed and recommissioned. In the South, a slightly smoother transition [31] is installed. With proper launch, η is matched throughout. The sensitivity of the betatron motion from systematic gradient errors is reduced, but random erect and skew quadrupole errors still cause some blowup and cross-coupling, although more gradual in nature [see fig. 8 (a)]. Cures involve empirically varying phases in troubled areas to reduce the coherence in the buildup, much as tunes are adjusted away from resonances in circular machines. Such a *detune-fix* [32] is shown in fig. 8(b) where blowup was reduced by disconnecting the FD-imbalance, thus causing about a 1° per cell difference between X and Y phases.

Another planned [33] cure consists of exciting harmonic [34,35] gradient perturbations with a pattern of trim windings, to suppress damaging Fourier components in the errors at twice the betatron frequency. Although this will be required for the final optimization, beams are now routinely transported to the Final Focus with distortions which can be absorbed by optical matching there.

FINAL FOCUS

Summary of Optics Goals [11-13]

The primary goal is to focus both beams to a small transverse size of about 2 μm. This would be easy for small enough transverse emittances and energy spreads. The limiting effect is the *chromaticity* of the focusing system needed to demagnify the beams, which as was described in the Arc causes both sine and cosine-like trajectories to be shifted for different energies. For a simplified Final Focus (see fig. 9), the contribution to the betatron spot size from *chromatic aberration* is $\sigma_{chrom} \simeq 2l^*\sigma_E\sigma_\theta^*$, where σ_θ^* is the IP angular size and l^* the distance from the principal plane of the final lens system to the IP (a factor two is put in since at least two lenses are used to focus both planes). The effect would be tolerable if $\epsilon\sigma_E \leq \sigma_x^{*2}/2l^*$. This is not the case in the SLC Final Focus, where $\sigma_x^* \simeq 1.5$ μm, $\epsilon \simeq 3\ 10^{-10}$ mrad, $\sigma_E \simeq 0.002$ and $l^* \approx 5$ m, amounting to $\sigma_{chrom}^* \simeq 4$ μm.

The reduction in luminosity, computed [36] by averaging the usual expression over the two beam's energy distributions, is shown in fig. 10 (dotted lines) versus β^*, for the as-built Final Focus. With $\sigma_E = 0.002$ and $\beta_{opt}^* \simeq 1.5$ cm, the luminosity is reduced by a factor 3.5.

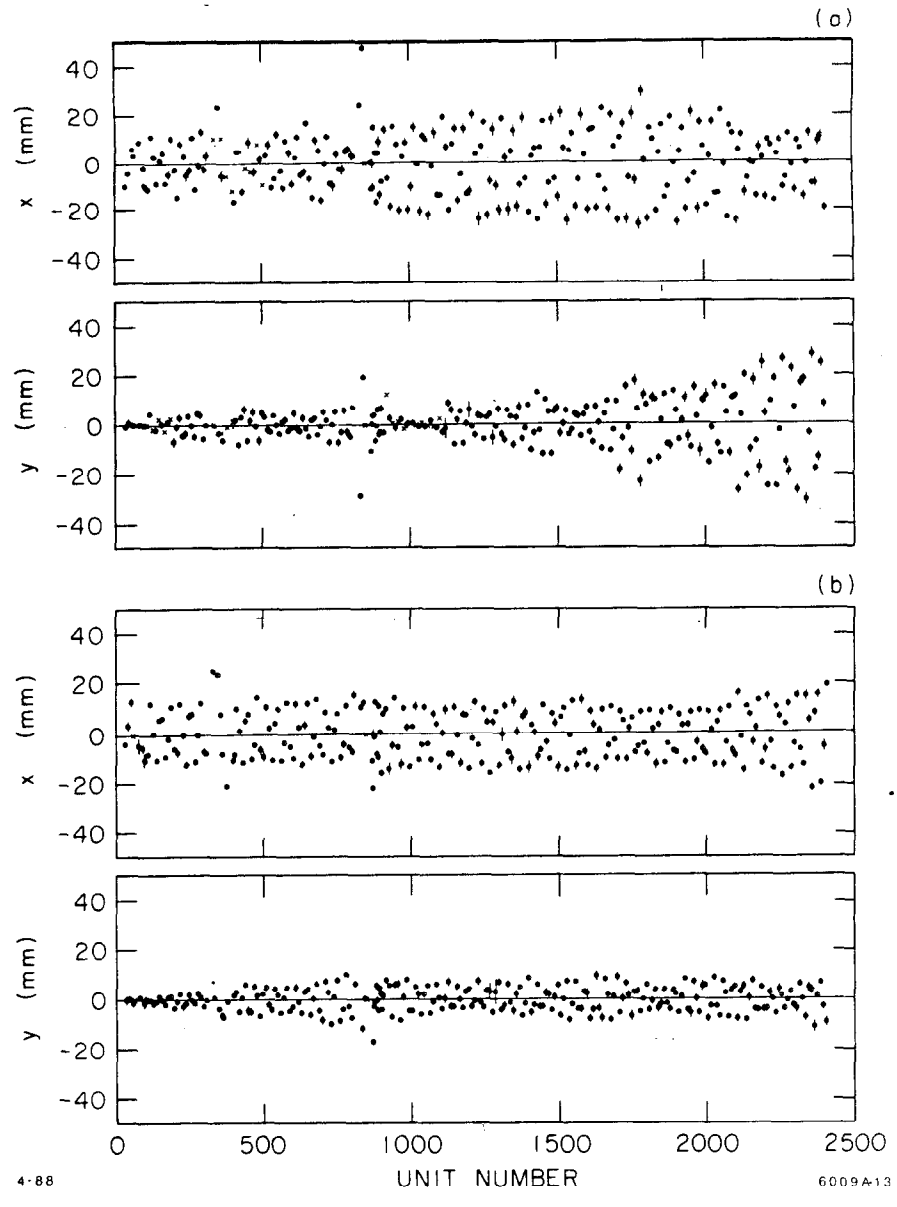

Fig. 8. Growth of a betatron oscillation in the South Arc, before (a) and after (b) *detune-fix*.

A Chromatic Correction Section (CCS) is introduced upstream of the final lens to cancel this effect. In a simplified CCS, two dipoles of strength B, separated by $2l_{ccs}$, are imaged by a quad with focal length $l_{ccs}/2$ (see fig. 9). Near the quad is a sextupole of strength S, through which rays with energy deviation δ_E travel off-axis. This produces a stronger overall quad for $\delta_E > 0$, which must here offset the weaker focusing in *both* final and CCS quads. The largest contribution to the chromaticity is from the final lens. Equating it to the effect from the sextupole, we find that $S \propto R_l/MB$, where $M = l^*/L$ and $R_l = l^*/l_{ccs}^2$.

Additional aberrations in θ^2 and δ_E^2, as in the Arc, are suppressed by pairing the sextupoles π phase-shift apart and by assuring sequential symmetry for η. The section departs, however, from a pure second-order achromat through the bends, placed where angular spreads are large to minimize synchrotron radiation emittance growth. The real system [11-13], designed to focus achromatically in both planes, is

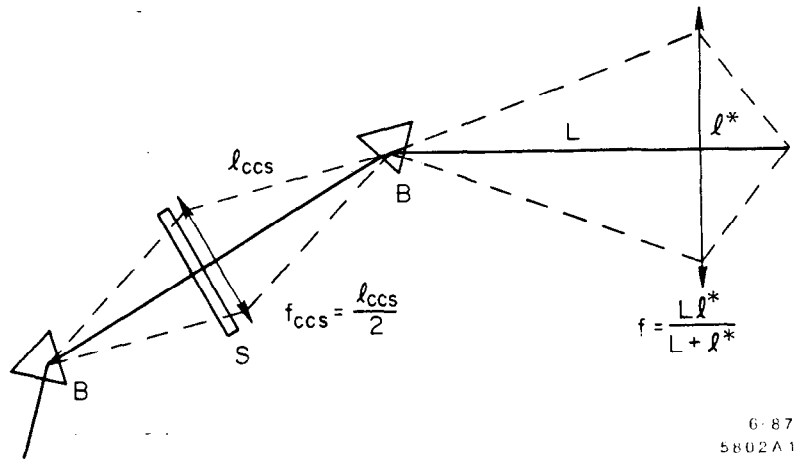

Fig. 9. A simplified Final Focus System.

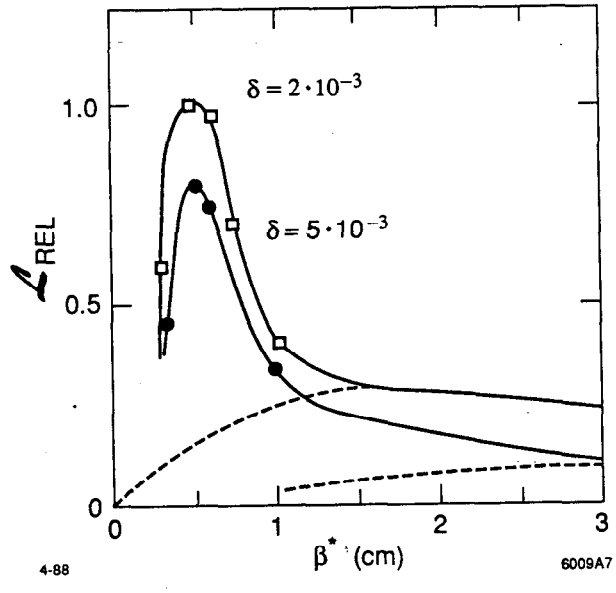

Fig. 10. Luminosity loss versus β^*, with second-order chromatic correction (solid line) and without (dotted line).

telescopic and uses triplets instead of lenses. This suppresses [12,37] the cosine-like terms in $x\delta_E$,$y\delta_E$ and minimizes [13] the sine-like chromaticities in $\theta\delta_E$,$\phi\delta_E$, while demagnifying in both planes. Two interleaved sextupole families are used to correct both planes. Coupling effects between these can enhance third-order aberrations and must be minimized. If we neglect the final lens system, the three dominant terms in $\theta\delta_E^2$, $\theta^2\delta_E$ and θ^3 scale like $S^2B^2\sigma_E^2\sigma_\theta^* M$, $S^2B\sigma_E\sigma_\theta^{*2}M^2$ and $S^2\sigma_\theta^{*3}M^3$. Substituting for the sextupole, we get $\frac{R_1^2\sigma_E^2(\epsilon/\beta^*)^{1/2}}{M}$, $\frac{R_1^2\sigma_E(\epsilon/\beta^*)}{B}$ and $\frac{R_1^2M(\epsilon/\beta^*)^{3/2}}{B^2}$. For given phase-space volume, space constraints and desired β^*, the overall effect from these aberrations can be minimized by adjusting [1] M,B and S to balance them out.

The overall effect of the chromatic correction is shown in fig. 10 (solid line), from MURTLE [38]). As expected, removing all second-order aberrations raises L^{max} and reduces β_{opt}^*. The optimum is now limited by leftover third-order terms. As it is more peaked, it is also more sensitive to proper matching.

The entire system is shown in fig. 11. Two additional sections are included to match the Arc η and β-functions. Extraction of the opposing beam is also provided, in the β-match section, through a pulsed magnet and septum.

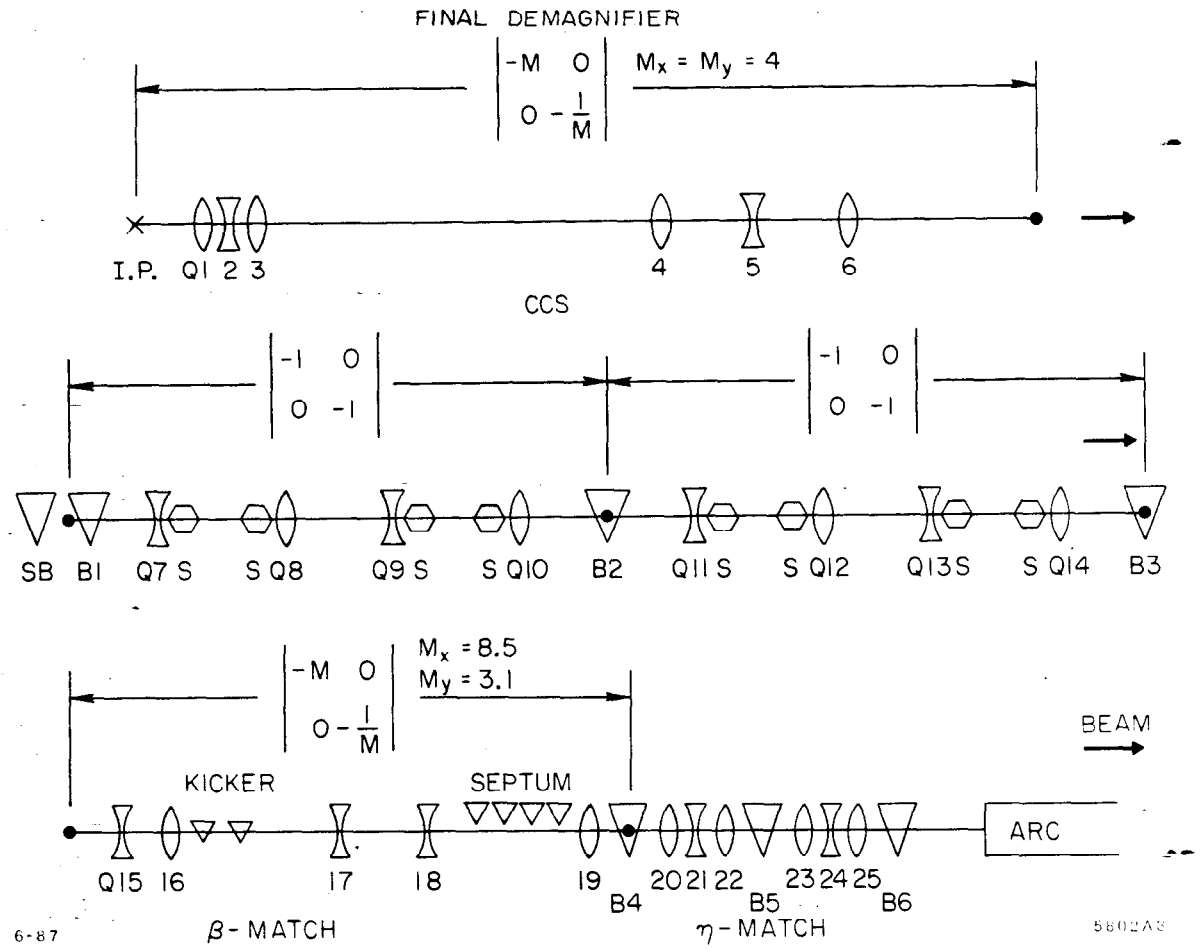

Fig. 11. Schematic of the Final Focus System.

Variable Matching [36]

Both the volume and shape of the input phase-space can be perturbed by imperfections. Errors generated within the Arc are in principle stable, but the linac is more variable as the energy profile depends on the set of klystrons used to accelerate. This set can change as faulty ones are exchanged for spares, and the phase-space then varies unless the focusing is rescaled. Also, mismatch at the Linac input *filaments* through the chromaticity of the Linac lattice, if and when the energy spread is minimized at the end but not locally. Good matching in the Linac is especially important at high current, when large local energy spreads are used to stabilize [39] transverse wakefields. Ongoing efforts have improved controls in the Linac, but some variations still exist. These are then further amplified by distortions in the Arcs.

The Final Focus includes adjustable matching mainly for *static* errors accumulated upstream. In establishing a proper setup and while work on stability proceeds, this matching is also used to some extent as an overall variable feedback. This is not optimal for several reasons, as will be explained.

Enhanced emittances or energy spread are uncorrectable. Larger $\epsilon_{x,y}$ are a major concern for both luminosity and detector backgrounds. The purely optical damage is slightly worse than linear because of third-order aberration, giving [36] $L \propto \epsilon^{-\frac{4}{3}}$ for $\beta^*_{opt} \propto \epsilon^{\frac{1}{3}}$. Third-order effects from a larger σ_E are apparent in fig. 10, showing close to linear loss with σ_E and weak dependance on β^*. The tolerance on σ_E is about 0.005.

Optical distortions in the Arcs are mostly linear [40] and are correctable within some bounds. The primary set enhances σ^* by correlating positions with angles or with δ_E, amounting to axially offsetting the waists, x-y coupling ($x\phi$ or $y\theta$ terms) or anomalous $\eta_{x,y}$. The waist must be corrected to within the depth of field $\beta^* \simeq 0.5$ cm; $\eta_{x,y}$ must be smaller than 1 mm. A second set enlarges σ^* by perturbing IP angular spreads ($< \theta^2 >$,$< \phi^2 >$, anomalous $\eta_{\theta,\phi}$ and $\theta\phi$ coupling terms). Smaller spread increases β^*, leading to $\mathcal{L} \propto 1/\beta^*$ from linear optics. Larger spread reduces β^*, but also enhances higher order contributions, leading to rapid loss. From fig. 10, β^* must be within $\pm 50\%$.

Optical corrections: In the design $\epsilon_x = \epsilon_y$ case, the betatron phase-space can [36] be perturbed in only six independent ways. With the four dispersions, $\eta_{x,\theta,y,\phi}$, there are thus *ten independent distortions* in total. We represent them by those for which tolerances were given: the five IP angular sizes $< \theta^2 >$,$< \phi^2 >$,$< \theta\phi >$ and $\eta_{\theta,\phi}$, and the five correlations of IP positions to angles and energy $< x\theta >$, $< y\phi >$, $< y\theta >$ (or $< x\phi >$) and $\eta_{x,y}$. The Final Focus is equipped to correct these ten distortions. If $\epsilon_x \neq \epsilon_y$, the six betatron variables chosen do not fully describe [41] the phase-space and more correction elements are needed.

Dispersion is corrected in the η-match with four quads [13], installed in pairs $\pi/2$ apart, to control spatial and angular terms, respectively. Each pair consists of an erect and a skew quad to correct both planes. Naturally orthogonal for small input error, these correctors are coupled if it is large. Correction range is mainly limited by quad strengths, but some values of the input make the correction singular; for example, when $\eta^{anomalous}_{x,\theta}$ exactly cancels $\eta^{lattice}_{x,\theta}$. In this case, control is required upstream.

Correctors for betatron mismatch straddle the CCS. The three angular terms are adjusted upstream of the CCS with two erect and one skew quad. The three waist terms cannot be adjusted there independently of the angular terms. They are taken out with trims on two of the final quads and a second skew quad. Correction range is about $\pm 50 \times \beta^*$ for waists and a factor four in either direction for angle spreads. The scheme is shown in fig. 12.

Optically, the system can correct as large as factor three mismatches. In practice, large distortions are not handled well for two reasons.

The first is lack of orthogonality in the corrections resulting from severe space limitations. The three waist corrections can internally be made orthogonal [42], but all the others are coupled. This is the case for the two skew quadrupoles, for the sextupoles, which must be refitted after betatron matching as the correctors straddle them, and for the extraction, which straddles two of the variable lenses and must be reoptimized after betatron matching. The η-correction is also non-orthogonal to the β-match, particularly [43] for magnified or demagnified optical configurations. Operationally, modest variations are amplified by distortions remaining in the Arcs, and can require extensive reoptimization. Effort is therefore directed both towards improving the Arc lattice and towards correcting variations in the Linac, to avoid feeding back on them in the Final Focus.

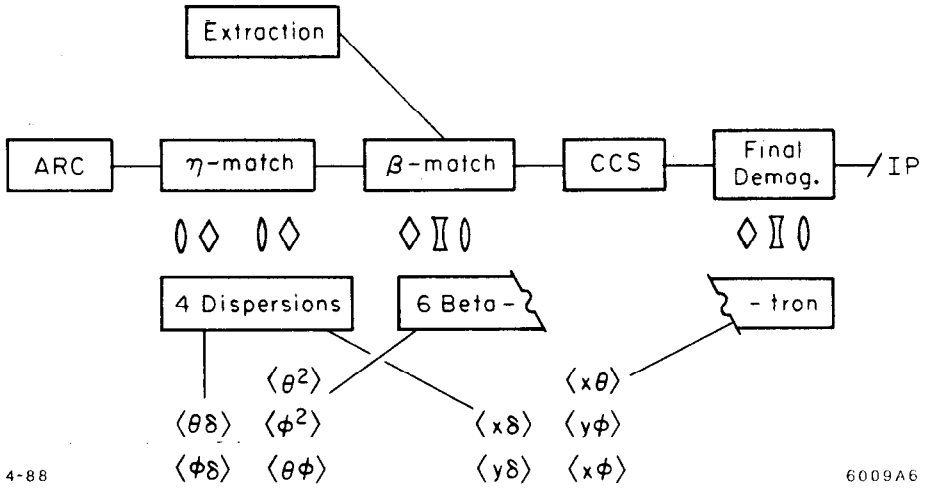

Fig. 12. Optical matching in the Final Focus System.

The second reason is the background induced in the detector by beam-tails impinging on tight apertures at the injection to the Final Focus. These apertures as well as some adjustable collimators are upstream of the main matching elements. Harmful background from hits on these apertures can result from otherwise correctable distortions. Recent experimental work [44] indicates more stringent tolerances on input errors from this viewpoint. This may require introducing further optical corrections in the Arcs, and redeployment of some collimators upstream.

Tuning Strategy and Initial Results

In this section, we describe single-beam optical adjustments in the Final Focus. Combined adjustments of several SLC systems to produce and maintain luminosity with tolerable background are ongoing and not described here. Similarly, two-beam tuning and steering methods are described elsewhere [45,46]. Some initial beam tests are reported.

We first match [47] η from the Arc. Strip-line beam position monitors are used to measure beam motion versus energy. This does not give position-energy correlations in the bunch if anomalous η exists where the energy is varied, but gives a good estimate if the Arc is (as expected) the dominant contributor. Using a model, we determine $\eta^{anomalous}_{x,\theta,y,\phi}$ from a least-square fit to the measurements and calculate the correction. An example of this is shown in fig. 13.

Trajectory errors within the Final Focus can also generate η at the IP. Correction is achieved by undoing some of the upstream match, although this also affects [43] waist-corrections and must be the result of a combined fit.

Betatron mismatch is best diagnosed near the IP, where angular and spatial sizes are naturally separated. The three angular terms, $< \theta^2 >$, $< \phi^2 >$ and $< \theta\phi >$, are first adjusted crudely looking at a nominally round spot on a high-β screen upstream of the Final Triplet. An example of this is shown in fig. 14, where the action of the upper skew quad is seen and where the beam has close to the design size.

This does not give β^* if ϵ is unknown. Also, if waist offsets are large, design size at the high-β screen does not correlate well with IP angular size. For better determination, spot sizes are measured at the IP, by scanning the beam across a thin 5 μm secondary emission wire target [48], as functions of the three waist

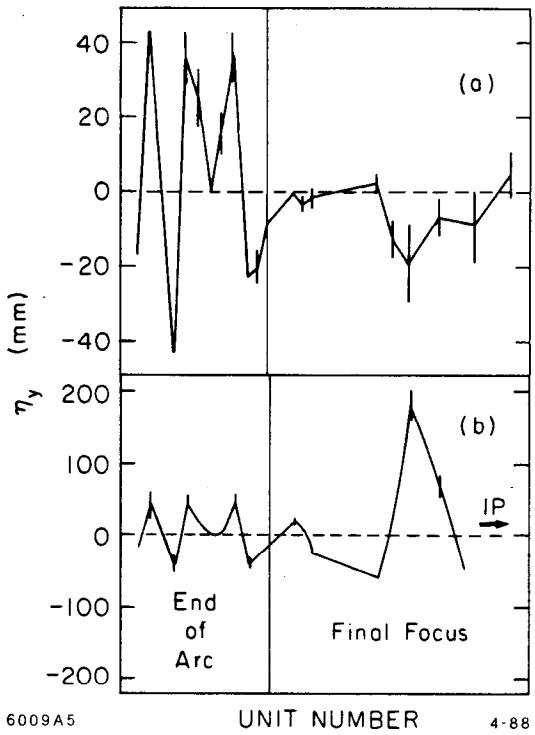

Fig. 13. On-line matching of the vertical dispersion function at the injection to the Final Focus. (b) shows mismatch before correction. (a) shows the effect of the correction. Please note the change of scale.

controls, starting with the second skew quad. Neglecting changes in IP angular spread, β^* and ϵ are found fitting $\epsilon\beta^* + \frac{\epsilon}{\beta^*}$ to the square of the beam size. Angular spreads are well determined from the parabolas branches, but both ϵ and β^* estimates suffer if the linear spot is not resolved. This arises through residual cross-coupling, only partially correctable for $\epsilon_x \neq \epsilon_y$, and through third-order aberration present before fully matching the β-function. Sextupoles must also be fitted in the perturbed lattice before scanning the waists, to maintain good second-order correction. Measured ϵ and β^* values serve as input for fitting the six β-matching quads towards design phase-space parameters. Both on-line and off-line models [47,49,50] are used. An empirical search around the calculated β^* is also planned for optimization.

Relatively small spots were sometimes obtained originally by only scanning the waists. An example of this is shown in fig. 15, where a 5 μm spot was obtained, with sextupoles turned off all together. The phase-space had to be rather close to nominal for this to be possible. As input parameters changed, small spots did not always reproduce.

More recently, the tolerance to input variations has been widened by running with a $\beta^* = 3$ cm lattice, as a starting guess of the most probable angular spread correction needed. Also, improvements have been made on stability and matching upstream. Beams with smaller than 5 μm sizes are now relatively easy to reproduce for both electrons and positrons with only the three waist-scans.

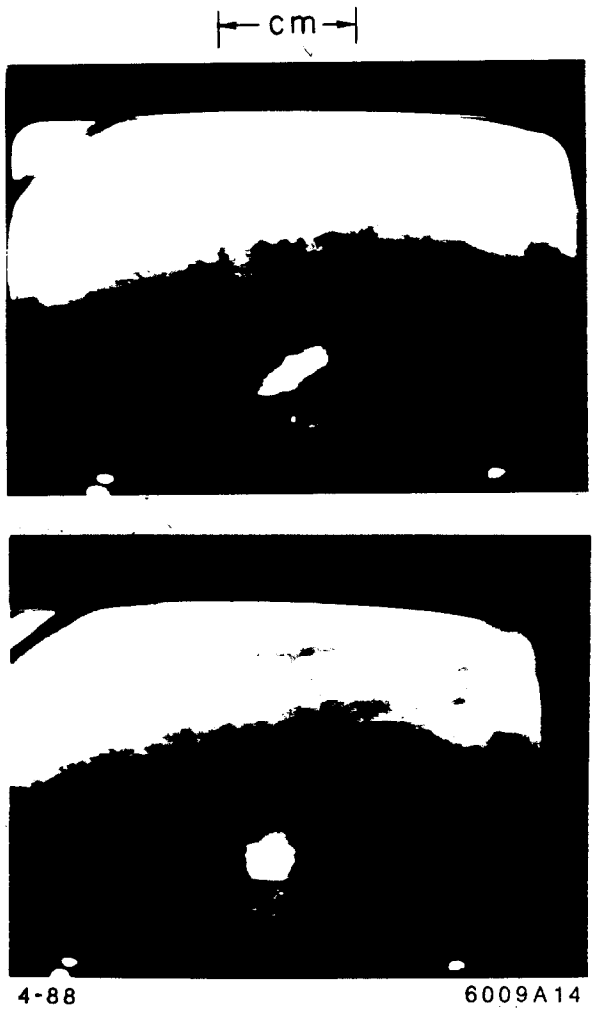

Fig. 14. Crude correction of cross-coupling in the IP angular spreads, looking at the tilt on a screen at the high-β point: (a) before correction; (b) after correction.

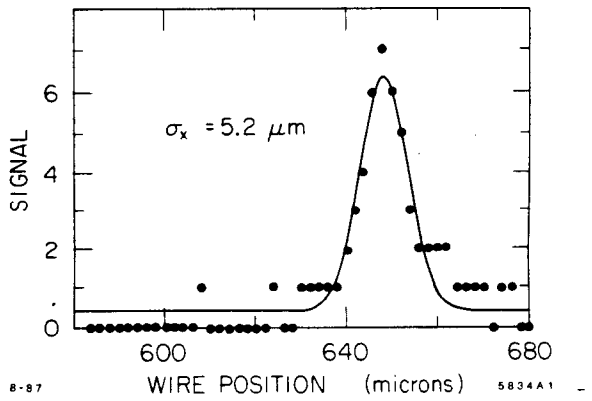

Fig. 15. First measurement of "small spot" at the IP.

SUMMARY STATUS AND NEAR FUTURE

Commissioning is now proceeding rapidly towards an initial low luminosity physics run. Both beams are routinely extracted onto their dumps, and reasonably small beam sizes are usually reproduced at the IP. Main priorities are phase-space controls and stability in the whole machine needed to maintain small spots, background reductions and general system reliability and operability. A shift towards operation has been made to assure more continuity in the commissioning and a more global approach towards stability and tuning issues. The Mark II detector, installed on the beamline during last year's shutdown, has been turned on a few times to help look at backgrounds. Studies indicate that collimators may have to be redeployed from the Final Focus to upstream places where beams can be comfortably trimmed without generating excessive muons in the detector. Also, enhanced optical matching in the Arcs through harmonic corrections is being considered for early installation, to help reduce distortions in the Final Focus. Extrapolating our recent rate of progress, and with some well-deserved luck, we hope to produce and detect a hundred Z^0 before Summer 1988.

ACKNOWLEDGEMENTS

I have profited interacting with numerous SLC and Mark II colleagues on several topics described here. New insight and progress have often resulted. Discussions with Karl Brown, Dave Burke, Roger Erickson, Ted Fieguth, Bill Ford, Andrew Hutton, Witold Kozanecki, Joe Murray, Nan Phinney, Dave Ritson, Lenny Rivkin, Marc Ross, Matt Sands, John Seeman, John Sheppard, Rae Stiening, Nobu Toge and many others, were both stimulating and interesting. I have in particular enjoyed working with Karl Brown and David Ritson on optics problems in the Arcs and Final Focus. Dave and I collaborated on the tuning strategy for the Final Focus. I especially wish to acknowledge his contribution. At last, I wish to thank Karl for reading this paper and for suggesting several improvements.

REFERENCES

[1] *SLC Conceptual Design Report,* SLAC–Report–229, June 1980; *SLC Design Handbook,* December 1984; *Proceedings of the SLC Workshop,* SLAC–Report–247.

[2] B. Richter, Nucl. Inst. Meth. **136,** 47 (1976).

[3] B. Richter and R. Stiening, The SLAC Linear Collider—A Status Report, *Proceedings of the International Symposium on Lepton and Photon Interactions at High Energy* (Hamburg, Germany, July 1987).

[4] R. Stiening, *Proposed Parameter Specification for FY88,* April 1988.

[5] J. C. Shepphard et al., Commissioning the SLC Injector, *Proceedings of the Particle Accelerator Conference* (Washington, D. C., March 1987).

[6] G. E. Fischer et al., A 1.2 GeV Damping Ring Complex for the Stanford Linear Collider, *Proceedings of the Twelfth International Conference on High Energy Accelerators,* FNAL, 37 (1983).

[7] J. T. Seeman et al., Experimental Beam Dynamics in the SLC Linac, *Proceedings of the Particle Accelerator Conference* (Washington, D. C., March 1987).

[8] F. Bulos et al., Design of a High Yield Positron Source, IEEE Trans. Nucl. Sci. **NS–32,** 1832 (1985).

[9] S. Ecklund, The Stanford Linear Collider Positron Source, *Proceedings of the Workshop on Intense Positron Beams* (Idaho Falls, Idaho, June 1987).

[10] G. E. Fischer et al., Some Experiences from the Commissioning Program of the SLC Arc Transport System, *Proceedings of the Particle Accelerator Conference* (Washington, D. C., March 1987).

[11] R. Erickson, Final Focus Systems for Linear Colliders, *Proceedings of the U. S. Summer School on High Energy Particle Accelerators* (Batavia, Illinois, August 1984).

[12] K. Brown, A Conceptual Design of Final Focus Systems for Linear Colliders, *Proceedings of the U. S.–CERN Joint Topical Course: Frontiers of Particle Beams* (South Padre Island, Texas, October 1986).

[13] J. J. Murray et al., The Completed Design of the SLC Final Focus System, *Proceedings of the Particle Accelerator Conference* (Washington, D. C., March 1987).

[14] R. Stiening, Status of the SLAC Linear Collider, *Proceedings of the Particle Accelerator Conference* (Washington, D. C., March 1987).

[15] J. T. Seeman and J. C. Shepphard, Status of the SLC, *Proceedings of the Workshop on New Developments in Particle Accelerator Techniques,* (Orsay, France, June 1987).

[16] A. J. Lankford, The Status of the SLAC Linear Collider and of the Mark II Detector, *Proceedings of the Seventh International Conference on Physics in Collision* (Tsukuba, Japan, August 1987).

[17] W. Kozanecki, Progress Report on the SLAC Linear Collider, *Proceedings of the International Europhysics Conference on High Energy Physics* (Uppsala, Sweden, June 1987).

[18] R. D. Ruth, The Status of the SLC, *Proceedings of the ICFA Seminar on Future Perspectives in High Energy Physics* (Upton, New York, October 1987).

[19] M. A. Allen et al., Performance of the SLAC Linear Collider Klystrons, *Proceedings of the Particle Accelerator Conference* (Washington, D. C., March 1987).

[20] S. Kheifets et al., Beam Optical Design and Studies of the SLC Arcs, *Proceedings of the Particle Accelerator Conference* (Washington, D. C., March 1987).

[21] M. Sands, *The Physics of Electron Storage Rings—An Introduction,* SLAC–121 Addendum (1979).

[22] M. Sands, *Emittance Growth from Radiation Fluctuations,* SLAC–AP–47 (1985).

[23] R. H. Helm and H. Wiedemann, *Emittance in FODO–Cell Lattice,* PEP–Note–303 (1979).

[24] R. Stiening, *Dynamic Beam Loading Compensation and Energy Spread in the SLC,* SLAC–CN–110 (1981).

[25] K. L. Brown, *A Second–Order Magnetic Optical Achromat,* SLAC–PUB–2257 (1979).

[26] B. Weng et al., SLC Arc Transport System–AG–Magnet Measurement and Performance, *Proceedings of the Particle Accelerator Conference* (Vancouver, B. C., Canada, May 1987).

[27] M. Sands, *Betatron Oscillations and Rolled Achromats,* SLAC–CN–355 (1987).

[28] K. L. Brown et al., SLAC–91, Rev. 2, May 1977.

[29] D. Ritson, private communication, June 1987.

[30] D. Ritson, BEAMSIM, private program.

[31] L. Rivkin and M. Sands, private communication, November 1987.

[32] N. Toge, private communication, March 1988.

[33] P. Bambade, *Harmonic Corrections in the Arcs,* in preparation.

[34] R. Stiening, *Focussing Errors in the SLC Linac Quadrupole Lattice,* SLAC–CN–161 (1982).

[35] T. H. Fieguth, *GIAT Committee Report,* October 1985.

[36] P. S. Bambade, Beam Dynamics in the SLC Final Focus System, *Proceedings of the Particle Accelerator Conference* (Washington, D. C., March 1987).

[37] K. L. Brown, private communication, June 1987.

[38] J. J. Murray and T. Fieguth, MURTLE, private program.

[39] K. Bane, Wake-Field Effects in a Linear Collider, IEEE Trans. Nucl. Sci. **NS–32,** 1662 (1985).

[40] K. L. Brown and R. V. Servranckx, *GIAT Committee Report,* February 1986.

[41] L. Rivkin, private communication, October 1987.

[42] P. S. Bambade, *GIAT Committee Report,* March 1987.

[43] B. Ford, private communication, April 1988.

[44] D. Burke, private communication, April 1988.

[45] P. S. Bambade and R. Erickson, Beam–Beam Deflections as an Interaction Point Diagnostic for the SLC, *Proceedings of the Linear Accelerator Conference* (Stanford, California, June 1986).

[46] G. Bonvicini et al., Beamstrahlung Monitor for SLC Final Focus Using Gamma Ray Energies, *Proceedings of the Linear Accelerator Conference* (Stanford, California, June 1986).

[47] C. Hawkes and P. S. Bambade, *First–Order Optical Matching in the Final Focus System of the SLAC Linear Collider,* in preparation.

[48] C. Field et al., *High Resolution Wire–Scanner for Micron Size Profile Measurements at the SLC,* SLAC–PUB–4605, to be published.

[49] W. Kozanecki, BETAMAT, private program.

[50] R. Servranckx and B. Ford, Flight Simulator for the Final Focus, private program.